

Electric Field Assisted Ion Exchange Strengthening of Borosilicate and Soda Lime Silicate Glass

Ali Talimian^{1,*}, Gino Mariotto², Vincenzo M. Sglavo^{1,3}

1. Department of Industrial Engineering, University of Trento, Trento 38123, Italy

2. Department of Computer Science, University of Verona, Verona 37134, Italy

3. Trento research unit, INSTM, Firenze 50121, Italy

* corresponding author

Abstract

In this study, we investigate the effects of electric field assisted ion exchange, EF-IE, on potassium ~~exchange~~ for sodium ~~ion exchanges in of~~ the soda borosilicate and soda lime silicate glasses. The results show that applying an electric field with the intensity of 1000 V cm^{-1} for few minutes produces an exchanged layer with a thickness comparable to the conventional chemical strengthening for 4h. There is a critical E-field that increases the mobility and, therefore, the diffusion coefficient of the potassium in the glasses. ~~The increase is, perhaps, related to the evolution of the glass structure due to the penetration of potassium ions under an E-field. Structural studies by micro Raman spectroscopies reveal that the structure of exchanged layer changes by subjecting to EF-IE: the changes can be explained by the theory of Cation-Induced Relaxation of Network, CIRON.~~

According to the Vickers' indentations, strong compressive stress is generated in the glass by EF-IE; however, the bending strength improvement is limited because of the presence of large surface defects and the stress distribution inhomogeneity.

* ali.talimian@unitn.it

Formatted

Formatted: Superscript

1 **Keywords:**

2 Electric field assisted ion exchange, chemical strengthening, soda lime silicate, borosilicate

3 **Introduction**

4 Glass has a fundamental role in different everyday-life applications such as electronics, cell
5 phones, solar cells, architectural components, and containers, although its typical brittleness.

6 Theoretically, glass is considered as the strongest human-made material; in practice, flaws
7 make it unreliable and weak from the mechanical point of view^{1, 2, 3, 4}. Among the several
8 reinforcement techniques proposed during the years, chemical tempering is a straightforward
9 and efficient technique for improving the mechanical performances of alkali silicate glasses^{2,}
10 ^{5, 6, 7}.

11 A compressive stress is produced on the glass surface by chemical tempering, or chemical
12 strengthening, which prevents and limits the formation and propagation of cracks. In a typical
13 process, small sodium or lithium ions are swapped for larger potassium ions diffusing into the
14 glass. Because of the diffusion nature of the process, treatments have to be carried out at
15 relatively high temperature for several hours; for this reason, stress relaxation can occur and
16 make strengthening less efficient than expected ^{1, 2, 3, 6, 8, 9}. The process can be enhanced by
17 applying ultrasonic waves, microwave heating or electric fields (E-Fields)^{10, 11, 12}. In particular,
18 electric field assisted ion exchange, EF-IE, has been ~~carried out~~conducted to modify the
19 refractive index of glass by producing a concentration of elements, like silver or chromium, for
20 optical devices ^{13, 14, 15, 16}.

21 The application of an E-field can change the governing mechanism of ion exchange from
22 diffusion to forced migration, thus accelerating the process and modifying the concentration
23 profiles, i.e., its shape and depth ^{3, 17, 18}. The EF-IE produces inhomogeneous stress distribution
24 in glass that be neglected in optical applications because of the limited depth of exchanged

1 layer. Nevertheless, the thick exchanged layer required for mechanical applications, which is a
2 must for improving the strength ^{5,6}, can change the geometry and, in extreme cases, it can lead
3 to sample failure. Therefore, controlling the depth of the ion-exchanged layer during the
4 process represents a critical and open issue. Nonetheless, particular geometries, i.e. cylinders,
5 can fulfill the required uniformity of compressive stress in the sample.

6 In the present work, we investigated the E-field assisted ion exchange in alkali borosilicate and
7 soda lime silicate glasses with specific attention to the generated potassium profile, the glass
8 structure evolution, and final strength.

9 Experimental procedure

10 Soda borosilicate (BS, Fiolax) and soda lime silicate (SLS, Ar-Glas) glass tubes with outer
11 diameter of 9.8 mm and the thickness of 0.6 mm and 1 mm, respectively, were bought from
12 SCHOTT AG to be used in the present work. The glass transition temperature was measured
13 by a differential scanning calorimeter (DSC) (DSC2010, TA Instruments, USA); glass powder
14 with a size lower than 200 μm was prepared by crushing the tubes in an agate mortar; then, the
15 powder was poured into an aluminium pas and placed in the DSC instrument. The samples
16 were heated up to 600°C with a heating rate of 10°C min⁻¹; the glass-transition temperature
17 was estimated according to ASTM E1356 norm¹⁹; The glass-transition temperature and the
18 chemical composition are reported in Table 1.

19 The tubes were ultrasonically cleaned in distilled water, washed with acetone and air-dried.

20 Ion exchange treatments (IE) were carried out in pure potassium nitrate, Haifa – Eurochemicals
21 (technical grade, $\geq 99.4\%$). Conventional chemical tempering was performed by a semi-
22 automatic furnace, TC 20A Lema, Parma, Italy, at 450°C for 4 h. The samples were kept 20
23 min over the salt bath before and after the treatment to avoid thermal shocks.

Formatted: Superscript

1 Electric field-assisted ion exchange treatments (EF-IE) were performed by a modified chemical
2 tempering furnace, TC 20S Lema, Parma, Italy. The salt bath temperature was kept at
3 $400\pm 10^\circ\text{C}$ during the treatment. The electrical field was varied between 100 V cm^{-1} to 2000 V
4 cm^{-1} by a power supply, DLM 600 Sorensen; the current density limit was fixed at 8 mA cm^{-2}
5 to prevent spark formation because of the salt electrolysis near the electrodes. The applied
6 voltage and current were monitored by a digital multimeter (DMM 2000, Keithley, Cleveland,
7 USA); ~~A~~a schematic of the setup used for samples preparations is drawn in Figure 1.



8 Borosilicate glass samples were subjected to the electric field for ~~duration as long as~~ 10 min,
9 while soda lime silicate tubes were treated by applying the field for 5 min because of the
10 shattering of samples, which is observed for longer treatments. The glass resistivity variation
11 against the applied electric field was measured by 4-point probe configuration and using time-
12 variant E-fields. The applied voltage was increased step by step, 5 V at each level, and dwelling
13 time of 5 s. The electrodes resistivity in the salt was measured as a function of the electric
14 current; the interference of electrodes, associated with salt electrolysis, was measured and
15 removed from the recorded data according to the following steps. First, the variations of the
16 electrode's resistance were estimated as a function of electric current until the formed passive
17 oxide layer on the electrodes is destroyed, and the resistivity drops. Then corresponding
18 resistance to the electrodes is removed from the experimental data. The influence of generated
19 gas can be neglected because of its limited production rate due to the applied current density
20 limit (8 mA cm^{-2}).

21 The mechanical strength of the samples was determined in air by four-point bending tests,
22 using spans of 18 mm and 40 mm and loading rate of 1.1 MPa s^{-1} . In this case, the samples
23 were produced using 1000 V cm^{-1} E-field until the amount of potassium sent into the glass was
24 comparable with that obtained by conventional ion-exchange at 450°C . The surface stress

Formatted: Superscript

1 generated by ion-exchange was estimated indirectly by Vickers indentations produced with
2 maximum load of 20 N and dwelling time of 15 s.

3 The potassium concentration profile was determined on the fracture surface of some tubes
4 fragments; such pieces were stuck on an aluminum disc by using conductive carbon paste and
5 then slightly coated with Pt-Pd alloy. The potassium concentration profiles were recorded by
6 scanning electron microscope (JEOL, JSM5500) equipped with an electron dispersion x-ray
7 spectrometer (EDS 2000, IXRF system, USA). The noise of the microprobe analysis was
8 filtered by smoothing it with a low pass filter and considering the potassium concentration of
9 the raw glass as the baseline, and afterward the experimental data was fitted using a modified
10 complementary error function¹⁸. The chemical composition on the glass surface was also
11 measured by EDS on the tubes before and after ion exchange.

12 Micro-Raman analysis was carried out  room temperature under ~~the~~ excitation of 514.5 nm
13 line of Ar-Kr gas laser.  spectra were collected from two different points of the samples
14 treated under E-field of 2000 V cm⁻¹, using the same experimental setup described in a previous
15 work²⁰. The spectra collected from the region that underwent ion-exchange near the surface of
16 glass are called "Edge". The other group of spectra was collected from an area in the middle of
17 glass, which has been not affected by ion exchange, is called "Bulk". ~~surface layer, underwent~~
18 ~~ion exchange, and the region unaffected by the exchange were called "Edge" and "Bulk",~~
19 ~~respectively.~~ The background of each spectrum was removed, and the spectrum was filtered to
20 eliminate the high-frequency noise²¹. ~~The peaks corresponding to vibrational modes of silicon-~~
21 ~~oxygen tetrahedra occurring in the wavenumbers of 850 to 1300 cm⁻¹ were fitted, and the peak~~
22 ~~integrals were used to calculate the relative distribution of the glass former units.~~

1 Results

2 Figure 2 shows the current density as a function of time in BS samples subjected to the E-fields
3 up to 2000 V cm⁻¹ with a current density limit equal to 8 mA cm⁻²; the treatments were
4 conducted in a molten potassium nitrate bath kept at 400±10°C. The current density, gradually
5 decreasing, is larger for higher applied fields. The current limit is achieved under an electric
6 field of 2000 V cm⁻¹. The current density is proportional to the E-field intensity and the inverse
7 of glass resistance; one can conclude that the current density decrease is due to the larger
8 resistance of the exchanged surface layer²².

9 The evolution of current density with time for SLS tubes, which are treated with the same
10 condition to BS glass, is reported in Figure 3. The behavior is quite similar to that observed in
11 borosilicate glass although the current limit is reached at 1000 V cm⁻¹. SLS glass contains more
12 alkali ions compared to BS ~~one-tubes~~ and, therefore, its conductivity and current density are
13 higher^{23, 24, 25}. This probably can account for the lower E-field at the current limit.

14 The molar ratio between potassium oxide and the total amount of alkali oxides (Na and K),
15 $K_2O/(K_2O+Na_2O)$, on the glass surface after EF-IE ~~carried-out~~ conducted under 1000 V cm⁻¹ is
16 shown in Table 2. The molar ratio of the raw glass and of tubes ~~simply-only~~ immersed in the
17 salt at 450°C for 5 min or treated by conventional ion exchange is shown for comparison. We
18 see that ~~potassium completely replaces sodium~~ sodium is completely replaced with potassium
19 on the external surface of EF-IE samples. A limited amount of potassium can be detected on
20 the inner surface of the glass, which is probably related to the limited diffusion of potassium
21 into the glass during the process^{26, 27}.

22 The potassium concentration profiles measured in BS samples subjected to EF-IE are shown
23 in Figure 4; the experimental data ~~was-were~~ smoothed and fitted by a modified complementary
24 error which will be discussed later on (Eq. 1). The curves resemble a step-like profile and the

Formatted: Superscript

Formatted: Superscript

1 depth increases with the applied E-field. The profiles can be divided into three main regions: a
2 first region, where potassium is constant and maximum, is followed by a second one where the
3 concentration suddenly decreases ~~to the raw glass situation amount~~. The exchanged layer
4 thickness reaches 15 μm after subjecting to E-field of 1000 V cm^{-1} for 600 s, which is
5 considerably deeper than the layer produced by conventional ion exchange at 450°C for 4 h,
6 shown in Figure 4.-

7 Figure 5 shows the potassium concentration profiles in SLS, the shape being similar to that
8 revealed in BS glass. In this case, the E-field with the intensity of 100 V cm^{-1} is not strong
9 enough to produce the constant concentration zone in 300 s. By applying E-fields stronger
10 than 500 V cm^{-1} , it is possible to produce an exchanged layer with a depth comparable to that
11 obtained by chemical strengthening at 450°C for 4 h, equal to $\approx 15 \mu\text{m}$.

12 The potassium concentration, $C_K(x,t)$, reported in Figure 4 and Figure 5 can be fitted by a
13 modified complementary error function as suggested in a previous work ¹⁸:

$$14 \quad C_K(x, t) = \frac{C_K^S}{2} \operatorname{erfc}\left(\frac{x - \left(\frac{DEt}{k_B T}\right)}{2\sqrt{Dt}}\right) \quad (1)$$

15 where x is the distance from the surface, t the time ~~and t are the distance from the surface and~~
16 ~~time, respectively,~~ C_K^S the surface concentration, D the diffusion coefficient of potassium. E
17 is the E-field intensity, T the absolute temperature and k_B the Boltzmann constant.

18 The diffusion coefficient, estimated by Eq. 1 for different applied E-Fields, is shown in Figure
19 6. For BS glass ~~it the coefficient~~ is around $6 \times 10^{-12} \text{ cm}^2 \text{ s}^{-1}$ for E-field up to 1000 V cm^{-1} ; then it
20 increases up to $12 \times 10^{-12} \text{ cm}^2 \text{ s}^{-1}$ ~~for E-field with intensity of when~~ 2000 V cm^{-1} is applied.- The
21 diffusion coefficient for SLS glass is larger ~~for SLS glass than BS samples; the coefficient it~~ is
22 around $10 \times 10^{-12} \text{ cm}^2 \text{ s}^{-1}$ ~~for very limited E-field (up to 200 V cm^{-1})~~ for the E-fields of 100 and
23 200 V cm^{-1} . We see that the coefficient increases with the applied E-field increase and it

Formatted: Superscript

1 ~~becomes ; then, it increases up to~~ $\sim 20 \times 10^{-12} \text{ cm}^2 \text{ s}^{-1}$; when the E-field is at 1000 V cm⁻¹ or
2 larger.

3 ~~—~~The diffusion coefficient is related to the mobility of ions, μ , through Einstein relation,
4 $D = \mu k_B T$. Therefore, the different ion mobility in the two considered glasses can be accounted
5 for explaining the observed differences in the diffusion coefficient.

6 Figure 7 shows the glass resistivity evolution as a function of the “actual E-field,” which is
7 estimated by removing the interference of electrodes. We see that the resistivity reaches a
8 constant value for limited E-field intensities in SLS glass, while it is an increasing function of
9 the E-field for BS glass; this is probably related to the different required activation energy for
10 diffusion and structural evolution of glasses. It must be mention that the BS behavior might
11 change under stronger E-field which can not be applied by using the mentioned -power supply.
12 The BS glass behavior under strong E-fields is a fundamental question needed to be answered.

13 Typical Vickers indentation patterns produced using load of 20 N are shown in Figure 8. The
14 compressive stress generated by ion exchange at 450°C for 4 h inhibits the crack propagation²⁸.
15 ²⁹. In glasses subjected to EF-IE, a relatively high compressive stress is generated on the surface
16 that prevents also the nucleation of cracks ^{30, 31}.

17 The bending strength of samples subjected to EF-IE and conventional ion-exchange is reported
18 in Table 3. Ion exchange clearly improves the mechanical resistance of the glasses. The BS
19 glass contains less sodium than SLS (Table 1); therefore, surface compression produced by IE
20 in BS is lower than in SLS. The strength of BS samples subjected to EF-IE is larger than in
21 conventionally treated ~~ones~~ samples. Conversely, for SLS tubes, EF-IE is less efficient than
22 conventional treatment, if we consider the final strength as a gauge of ion-exchange efficiency.

23 Additional features regarding the strength can be pointed out from the Weibull distributions
24 shown in Figure 9; the strength corresponding the failure probability, F, of 63.2% which is
25 known as the characteristic strength, is also reported in the plots. The characteristic strength of

1 BS glass increases from 72 MPa to 121 MPa after ion exchange; EF-IE improves the
2 characteristic strength a bit more, up to 141 MPa although failure resistance is more scattered.
3 Conventional ion exchange is also beneficial for SLS tubes, the characteristic strength
4 increasing from 420 MPa to 133 MPa, much more than EF-IE.

5

6 Discussion

7 The chemical strengthening efficiency depends on the stress production by stuffing larger
8 potassium ions into the glass. The EF-IE produces potassium concentration profiles with the
9 same depth as conventional ion exchange and a slightly higher K concentration. One may
10 expect that the EF-IE strengthening is more efficient than the conventional strengthening
11 because of the larger compression on the surface, as we can see in the case of BS glass.
12 Conversely, the SLS tubes treated by EF-IE show significantly lower strength compared to the
13 SLS samples treated by conventional ion exchange strengthening, but EF-IE strengthening of
14 SLS tubes is not as influential as that expected from BS samples, especially when it is compared
15 with conventional ion exchange strengthening. The distinction between the ion mobility and
16 the diffusion of ions, which is probably related to the structural evolutions, may be accounted
17 for the limited improvement of SLS glass using EF-IE.

18 E-field pushes the alkali ions into the glass surface and an E-field, strong enough, can also
19 change the governing mechanism of mass transfer. This occurs for example, in SLS samples
20 treated under E-field in excess of 100 V cm^{-1} (Figure 2) sodium ions being completely replaced
21 by potassium.

22 Ingram et al. have reported that the exchanged layer has a higher resistivity compared to the
23 raw glass^{32, 33}; consequently, the glass resistivity increases by increasing the depth of
24 exchanged layer and the current density decreases. The formation of an exchanged layer, which

1 is more resistive, generates an inhomogeneous distribution of the E-field in the glass, the inner
 2 surface being subjected to a weaker E-field; this is responsible for the limited potassium
 3 diffusion into the glass on the inner surface of tubes (Table 2). The glass resistivity is the
 4 representative of the mobility of alkali ions under E-fields and, hence, the diffusion coefficient.
 5 The glass subjected to ion exchange can be considered as a bilayer material composed of bulk
 6 glass (i.e. the raw glass) and the exchanged layer. The ~~resistivity-resistance~~ resistivity can be described
 7 by an equivalent electrical circuit consisting of two ~~resistances-resistors~~ resistors in series; a schematic
 8 drawing of the circuit is shown in Figure 1210. The total ~~resistivity-resistance~~ resistance of sample, R_{total} ,
 9 is a function of each layer thickness and resistivity, which can be expressed as:

$$R_{total} = xR_{exch} + (1 - x)R_{bulk} \quad (2)$$

11 where R_{exch} and R_{bulk} are the ~~resistivity-resistance~~ resistances of the exchanged layer and of the bulk,
 12 respectively. x is the ratio between the exchanged layer and the glass thickness. The ~~resistivity~~
 13 resistance of the exchanged layer can be considered constant because of the constant
 14 concentration of potassium; therefore, the ~~resistivity-resistance~~ resistance of the exchanged layer and the
 15 total glass ~~resistivity-resistance~~ resistance can be calculated as:

$$R_{exch} = R_{bulk} + \Delta R \quad (3)$$

$$R_{total} = R_{Na} \left(x \frac{\Delta R}{R_{Na}} + 1 \right) \quad (4)$$

18 Considering the actual thickness of exchanged layer ~~actual thickness~~, which is less than one
 19 percent of the overall glass thickness, the influence of the exchanged layer in Eq. 4 can be
 20 neglected and, therefore, the ~~resistivity-resistance~~ resistance of glass can be assumed equal to the
 21 resistivity of the bulk glass subjected to ion exchange. At constant temperature, the resistivity
 22 of glass containing only monovalent cations is a function of the E-field E, and the drift
 23 velocity v, of cation^{4, 34}:

$$R = \varphi \frac{E}{v} \quad (5)$$

1 where φ is a proportionality constant depending on the mobility of ions which can be be
2 estimated from:

$$\varphi = \frac{CF^2k_B}{RTe} \quad (6)$$

4 where v is the drift velocity of the charge carriers in the glass, F is the Faraday's constant, R
5 the perfect gas constant, T temperature, C the ratio of charge carriers (sodium ions) n , over the
6 total amount of mobile cations, N_{\pm} ; C can be considered equal to 1 here. e is the electron
7 charge= $1e$, k_B Boltzmann constant. Due to the constant temperature of treatments, φ can be
8 considered constant.

9 According to Eq. 5, glass resistivity is a linear function of the applied E-field unless the drift
10 velocity of ions changes non-linearly with the E-field, which accounts for non-ohmic behavior.

11 Figure 6 shows that the resistivity of SLS glass becomes constant at a certain E-field.

12 Conversely, the resistivity of BS continuously increases although with decreasing rate. This is
13 indicative of a non-linear increase of drift velocity with E-field. Similar behavior has been
14 previously reported in silver-containing glasses subjected to E-field, silver clusters producing
15 channels for ion conduction^{35, 36, 37, 38}. The formation of such channels is probably responsible

16 for the larger drift velocity and, therefore, for the abrupt increase of potassium diffusion
17 coefficient at certain E-field as shown in Figure 6. The movement of larger potassium ions via

18 sodium sites in the silicate glass structure might occur with breaking and rearranging of the bonds
19 through cation-induced-relaxation-of-network (CIRON) as proposed by Ingram et. al. It is
20 known that the alkali ion transport through the glass occurs by rearranging the Qn species^{22,}

21 ³⁹. Vareshneya A.K. suggested that the movement of invading potassium ions and the
22 accommodation of them in the sodium sites occur by bending or stretching of the bonds
23 surrounding the host site beyond the strain limit. This causes a permanent change in the glass

24 structure that might be responsible for the facilitated ions mobility and, consequently, the
25 diffusion coefficient^{6, 22, 39}, which can be described as $Q_2+Q_4 \leftrightarrow 2Q_3$ (Table 4).⁴⁰. The new glass

Formatted: Justified

1 ~~structure contains more Q₃ species, which are probably oriented to facilitate the alkali ions~~
2 ~~movement. The E-field of sufficient intensity can provide the required energy for breaking and~~
3 ~~reforming of the bonds.~~

4 It is possible to observe the evolution of glass structure from comparing the Raman spectra
5 collected from the layer undergone the Na/K exchange, called edge, and the bulk glass, which
6 is not influenced by the invading potassium ions. In order to ease the comparison of the
7 collected spectra, the background noise and fluorescence are removed: Figure 11 shows the
8 final Raman spectra in the 800 to 1250 cm⁻¹ region. The peak envelope in this window is
9 corresponding to the region where the Raman peaks are mainly associated with the silicon-
10 oxygen stretching vibrations in silicate Q_n units⁴¹. This region is a convolution of different
11 peaks mainly corresponding to the Q₂, Q₃ and Q₄ species^{41, 42}. We see that the peak shape of
12 exchanged layer is different from the bulk in the BS sample which reveals a change of the
13 degree of connectivity of the glass network (concentration of Q_n units). In the case of SLS
14 glass, the location of the peak maximum shifts to the higher wavenumbers. Such changes of
15 Raman spectra unveil the generation of a new structure in the ion-exchanged layer. More
16 studies are required in order to get a clear picture of the structural evolution during ion
17 exchange and possible transitions such as phase separation particularly in the case of
18 borosilicate glasses. Phase separation causes an abrupt change in glass resistivity of samples
19 because of the production of two different phases (glasses); this phenomenon appears as a
20 spontaneous change in the current density curves of samples. Since the current density of
21 samples does not change in such a fashion, it is fair to state that no phase separations occur in
22 these treatments.

23 It seems that an E-field, sufficiently strong, can provide the required energy for the possible
24 structural modifications. The current passing through the glass can also increase the temperature
25 because of Joule heating and cause structural and stress relaxation^{39, 43}. Nevertheless, due to

1 the limited thickness of the tubes, 0.6 mm (BS) and 1 mm (SLS), the sample temperature can
2 be considered constant and in equilibrium with the molten salt, at a temperature below the
3 stress relaxation temperature. The limited cracking after Vickers indentations (Figure 9) also
4 confirms the presence of surface compression in samples subjected to EF-IE.

5 The strengthening efficiency depends on the amount of replaced alkali ions on the surface ^{2, 6};
6 since SLS glass has twice sodium than BS, one should expect larger compressive stress and
7 higher strength in the former; this matches reasonably with the obtained ~~experimental~~
8 ~~data~~ results from Vickers' indentations. It is worth mentioning that some original defects are
9 larger than the exchange layer and can not be completely “reinforced” by IE process; such
10 flaws are responsible for limited strength values and account for the small Weibull modulus
11 estimated for EF-IE samples. It should be noted that only the exterior surface of the tubes was
12 subjected to EF-IE; therefore, the influence of original defects on the interior surface is crucial.
13 This can be clearly observed in the limited Weibull modulus for BS glass treated by EF-IE.

14 According to Vickers indentations results (Figure 8), there is strong compression on the surface
15 of EF-IE samples and the thickness of the exchanged layer is comparable to that produced by
16 IE; one can conclude that the limited strength of SLS samples treated by EF-IE is rather ~~related~~
17 ~~to~~ correlates with the non-symmetric stress distribution along the thickness than ~~to a thin~~
18 ~~compression layer in the surface~~ ~~insufficient surface compression~~. As the outer surface is
19 strongly compressed, the inner one undergoes ~~under~~ a significant, if not huge, tension;
20 consequently, the glass becomes very vulnerable to the defects of the inner surface and during
21 bending tests, failure can start from the inner surface at relatively small loads. ¹¹ This also
22 explains the lower Weibull modulus calculated for samples treated by EF-IE.

1 Summary and Conclusions

2 Electric field assisted ion exchange, EF-IE, was used to accelerate replacing sodium ~~by~~with
3 potassium on the surface of soda-lime silicate and soda borosilicate glasses. EF-IE produces
4 step-like concentration profiles in glasses with a depth comparable to the conventional ion
5 exchange in a significantly shorter time. The diffusion coefficient of potassium in glass changes
6 when it is subjected to E-fields; it seems that there is a critical E-field that can increase the
7 mobility of ions significantly; this phenomenon needs to be studied in detail. ~~During the EF-IE,~~
8 ~~the glass structure changes by rearranging the Qn species according to $Q_2+Q_4 \leftrightarrow 2Q_3$; this~~
9 ~~facilitates the ion movement.~~ EF-IE produces a strong compressive stress on the surface of
10 glass that prevents crack nucleation during Vickers' indentation; however, in this study, the
11 strength augmentation is probably hindered by the presence of large surface defects.

12 The electric field assisted ion exchange can be used in principle to produce a strong
13 compressive stress in soda lime silicate and soda borosilicate glass; however, the process
14 should be accurately controlled. This requires a deeper look into the stress build-up of stress in
15 glass by EF-IE; moreover, procedures for balancing the residual stress such as inverting the
16 polarization should be proposed and investigated.

17 Acknowledgements

18 We appreciate the assistance of Dr. Marco Giarola for ~~the micro-Raman measurements~~his help
19 with the characterisation of samples.
20
21

References

1. D. J. Green, "Recent Developments in Chemically Strengthened Glasses," pp. 253-66. in 64th Conference on Glass Problems: Ceramic Engineering and Science Proceedings. John Wiley & Sons, Inc., 2008.
2. S. Karlsson, B. Jonson, and C. Stalhandske, "The technology of chemical glass strengthening - a review," *Glass Technol-Part A*, 51[2] 41-54 (2010).
3. A. Tervonen, B. R. West, and S. Honkanen, "Ion-exchanged glass waveguide technology: a review," *Optical Engineering*, 50[7] 71107 (2011).
4. A. K. Varshneya, "Fundamentals of Inorganic Glasses." Society of Glass Technology, (2006).
5. A. K. Varshneya, "The physics of chemical strengthening of glass: Room for a new view," *Journal of Non-Crystalline Solids*, 356[44-49] 2289-94 (2010).
6. A. K. Varshneya, "Chemical Strengthening of Glass: Lessons Learned and Yet To Be Learned," *International Journal of Applied Glass Science*, 1[2] 131-42 (2010).
7. R. Gy, "Ion exchange for glass strengthening," *Materials Science and Engineering: B*, 149[2] 159-65 (2008).
8. A. Rahman, M. Giarola, E. Cattaruzza, F. Gonella, M. Mardegan, E. Trave, A. Quaranta, and G. Mariotto, "Raman microspectroscopy investigation of Ag ion-exchanged glass layers," *J Nanosci Nanotechnol*, 12[11] 8573-9 (2012).
9. S. I. Sviridov and N. P. Eliseeva, "Field-assisted diffusion of potassium ions in sodium silicate glass," *Glass Physics and Chemistry*, 32[6] 604-11 (2006).
10. Z. Fathi, D. E. Clark, and R. Hutcheon, "Surface Modification of Ceramics Using Microwave-Energy," *Mater Res Soc Symp P*, 269 347-51 (1992).

Formatted: Normal, Indent: Left: 0 cm, First line: 0 cm

- 1 11. M. Abou-El-Leil and A. R. Cooper, "Fracture of Soda-Lime Glass Tubes by Field-Assisted
2 Ion Exchange," *Journal of the American Ceramic Society*, 61[3-4] 131-36 (1978).
- 3 12. M. Abou-El-Leil and A. R. Cooper, "Analysis of Field-Assisted Binary Ion Exchange,"
4 *Journal of the American Ceramic Society*, 62[7-8] 390-95 (1979).
- 5 13. T. Izawa, "Optical waveguide formed by electrically induced migration of ions in glass
6 plates," *Applied Physics Letters*, 21[12] 584 (1972).
- 7 14. K. Liu and E. Y. B. Pun, "K⁺-Na⁺ ion-exchanged waveguides in Er³⁺-Yb³⁺ codoped
8 phosphate glasses using field-assisted annealing," *Applied Optics*, 43[15] 3179-84 (2004).
- 9 15. A. Quaranta, E. Cattaruzza, F. Gonella, G. Peruzzo, M. Giarola, and G. Mariotto, "Field-
10 assisted solid state doping of glasses for optical materials," *Optical Materials*, 32[10] 1352-55
11 (2010).
- 12 16. S. Ali, N. Ali, Y. Iqbal, A. Samreen, Q. Hayat, K. Hayat, M. Ajmal, and M. J. Iqbal,
13 "Structural modifications induced in silicate glass by field-aided solid-state diffusion of gold
14 and chromium ions," *Journal of Non-Crystalline Solids*, 420 38-42 (2015).
- 15 17. J. Hazart and V. Minier, "Concentration profile calculation for buried ion-exchanged
16 channel waveguides in glass using explicit space-charge analysis," *Ieee J Quantum Elect*, 37[4]
17 606-12 (2001).
- 18 18. P. Mazzoldi, S. Carturan, A. Quaranta, C. Sada, and V. M. Sglavo, "Ion exchange process:
19 History, evolution and applications," *Riv Nuovo Cimento*, 36[9] 397-460 (2013).
- 20 19. A. International, "Standard Test Method for Assignment of the Glass Transition
21 Temperatures by Differential Scanning Calorimetry." in *Calorimetry and Mass Loss*, Vol.
22 E1356-08. West Conshohocken, PA, 2014.
- 23 20. A. Quaranta, A. Rahman, G. Mariotto, C. Maurizio, E. Trave, F. Gonella, E. Cattaruzza, E.
24 Gibaudo, and J. E. Broquin, "Spectroscopic Investigation of Structural Rearrangements in

- 1 Silver Ion-Exchanged Silicate Glasses," *The Journal of Physical Chemistry C*, 116[5] 3757-64
2 (2012).
- 3 21. Z.-M. Zhang, S. Chen, Y.-Z. Liang, Z.-X. Liu, Q.-M. Zhang, L.-X. Ding, F. Ye, and H.
4 Zhou, "An intelligent background-correction algorithm for highly fluorescent samples in
5 Raman spectroscopy," *Journal of Raman Spectroscopy*, 41[6] 659-69 (2010).
- 6 22. M. D. Ingram, J. E. Davidson, A. M. Coats, E. I. Kamitsos, and J. A. Kapoutsis, "Origins
7 of anomalous mixed-alkali effects in ion-exchanged glasses," *Glass science and technology*,
8 73[4] 89-104 (2000).
- 9 23. O. L. Anderson and D. A. Stuart, "Calculation of Activation Energy of Ionic Conductivity
10 in Silica Glasses by Classical Methods," *Journal of the American Ceramic Society*, 37[12] 573-
11 80 (1954).
- 12 24. M. Dubiel, B. Roling, and M. Fütting, "Ac conductivity and ion transport in K⁺-for-Na⁺
13 ion-exchanged glasses: exchange experiments below and above the glass transition
14 temperature," *Journal of Non-Crystalline Solids*, 331[1-3] 11-19 (2003).
- 15 25. B. Vessal, G. N. Greaves, P. T. Marten, A. V. Chadwick, R. Mole, and S. Houde-Walter,
16 "Cation microsegregation and ionic mobility in mixed alkali glasses," *Nature*, 356[6369] 504-
17 06 (1992).
- 18 26. A. I. Fu and J. C. Mauro, "Mutual diffusivity, network dilation, and salt bath poisoning
19 effects in ion-exchanged glass," *Journal of Non-Crystalline Solids*, 363 199-204 (2013).
- 20 27. R. J. Araujo, S. Likitvanichkul, Y. Thibault, and D. C. Allan, "Ion exchange equilibria
21 between glass and molten salts," *Journal of Non-Crystalline Solids*, 318[3] 262-67 (2003).
- 22 28. C. Anunmana, K. J. Anusavice, and J. J. Mecholsky, Jr., "Residual stress in glass:
23 indentation crack and fractography approaches," *Dental materials : official publication of the*
24 *Academy of Dental Materials*, 25[11] 1453-8 (2009).

- 1 29. P. Jannotti, G. Subhash, P. Ifju, P. K. Kreski, and A. K. Varshneya, "Influence of ultra-high
2 residual compressive stress on the static and dynamic indentation response of a chemically
3 strengthened glass," *Journal of the European Ceramic Society*, 32[8] 1551-59 (2012).
- 4 30. G. R. Anstis, P. Chantikul, B. R. Lawn, and D. B. Marshall, "A Critical Evaluation of
5 Indentation Techniques for Measuring Fracture Toughness: I, Direct Crack Measurements,"
6 *Journal of the American Ceramic Society*, 64[9] 533-38 (1981).
- 7 31. R. F. Cook and G. M. Pharr, "Direct Observation and Analysis of Indentation Cracking in
8 Glasses and Ceramics," *Journal of the American Ceramic Society*, 73[4] 787-817 (1990).
- 9 32. A. Dutta, T. P. Sinha, P. Jena, and S. Adak, "Ac conductivity and dielectric relaxation in
10 ionically conducting soda–lime–silicate glasses," *Journal of Non-Crystalline Solids*, 354[33]
11 3952-57 (2008).
- 12 33. M. D. Ingram, "Ionic conductivity and glass structure," *Philosophical Magazine Part B*,
13 60[6] 729-40 (1989).
- 14 34. P. Heitjans and S. Indris, "Diffusion and ionic conduction in nanocrystalline ceramics," *J*
15 *Phys-Condens Mat*, 15[30] R1257-R89 (2003).
- 16 35. P. K. Mukherjee, D. Dutta, S. Bhattacharyya, A. Ghosh, and D. Chakravorty, "Giant
17 Dielectric Permittivity in Aligned Silver Nanowires Grown within (AgI)(AgPO₃) Glasses,"
18 *The Journal of Physical Chemistry C*, 111[10] 3914-19 (2007).
- 19 36. B. Gee, M. Janssen, and H. Eckert, "Local cation environments in mixed alkali silicate
20 glasses studied by multinuclear single and double resonance magic-angle spinning NMR,"
21 *Journal of Non-Crystalline Solids*, 215[1] 41-50 (1997).
- 22 37. B. Gee and H. Eckert, "Cation Distribution in Mixed-Alkali Silicate Glasses. NMR Studies
23 by ²³Na–{⁷Li} and ²³Na–{⁶Li} Spin Echo Double Resonance," *The Journal of Physical*
24 *Chemistry*, 100[9] 3705-12 (1996).

- 1 38. B. Gee and H. Eckert, "²³Na nuclear magnetic resonance spin echo decay spectroscopy of
2 sodium silicate glasses and crystalline model compounds," *Solid State Nuclear Magnetic*
3 *Resonance*, 5[1] 113-22 (1995).
- 4 39. M. D. Ingram, M. H. Wu, A. Coats, E. I. Kamitsos, C. P. E. Varsamis, N. Garcia, and M.
5 Sola, "Evidence from infrared spectroscopy of structural relaxation during field assisted and
6 chemically driven ion exchange in soda lime silica glasses," *Physics and Chemistry of Glasses*,
7 46[2] 84-89 (2005).
- 8 40. C. Calahoo, J. W. Zwanziger, and I. S. Butler, "Mechanical–Structural Investigation of Ion-
9 Exchanged Lithium Silicate Glass using Micro-Raman Spectroscopy," *The Journal of Physical*
10 *Chemistry C*, 120[13] 7213-32 (2016).
- 11 41. E. Stavrou, D. Palles, E. I. Kamitsos, A. Lipovskii, D. Tagantsev, Y. Svirko, and S.
12 Honkanen, "Vibrational study of thermally ion-exchanged sodium aluminoborosilicate
13 glasses," *Journal of Non-Crystalline Solids*, 401 232-36 (2014).
- 14 42. P. Mcmillan and B. Piriou, "Raman-Spectroscopic Studies of Silicate and Related Glass
15 Structure - a Review," *B Mineral*, 106[1-2] 57-75 (1983).
- 16 43. J. Shen, D. J. Green, R. E. Tressler, and D. L. Shelleman, "Stress relaxation of a soda lime
17 silicate glass below the glass transition temperature," *Journal of Non-Crystalline Solids*, 324[3]
18 277-88 (2003).
- 19
20
21
22

Figure 1 Schematic of the experimental setup for sample preparation and the instrumentation for monitoring and controlling the electric field

Figure 2 Current density as a function of time in BS tubes subjected to different E-fields (current density limit: 8 mA cm^{-2}).

Figure 3 Current density as a function of time in SLS tubes subjected to different E-fields (current density limit: 8 mA cm^{-2}).

Figure 4 Relative potassium concentration profiles for BS tubes subjected to electric field-assisted ion exchange (EF-IE) at 400°C , and conventional ion exchange at 450°C for 4h

Figure 5 Relative potassium concentration profiles for SLS tubes subjected to electric field-assisted ion exchange (EF-IE) at 400°C , and conventional ion exchange at 450°C for 4h

Figure 6 Diffusion coefficient estimated for variable electric fields for samples treated at 400°C . (a) borosilicate, (b) soda lime silicate glass

Figure 7 Evolution of resistivity as a function of applied electric field for glasses immersed in potassium nitrate at 400°C ; The second x-axis presents the applied E-field regarding the power supply output voltage

Figure 8 Vickers indentations on glasses, borosilicate and soda lime silicate glass: (a) and (d) as cut, (b) and (e) conventional ion exchanged, (c) and (f) exchanged under E-field (2000 V cm^{-1})

Figure 9 Weibull distributions of : (a) BS; (b) SLS glass. Fitting lines used for the determination of Weibull modulus (m) and specific characteristic strength (reported values) are shown (F is the failure probability)

Figure 10 Equivalent circuit model of a glass subjected to electric field assisted ion exchange

Figure 11 Micro-Raman spectra of glasses subjected to EF-IE (2000 V cm⁻¹) in 800-1250 cm⁻¹ region: (a) borosilicate glass, (b) soda lime silicate glass

Table 1 Chemical composition and transition temperature of the glass tubes used in this work.

	Chemical composition (wt%)								Glass transition temperature
	SiO ₂	B ₂ O ₃	Al ₂ O ₃	CaO	MgO	BaO	Na ₂ O	K ₂ O	
Borosilicate (Fiolax)	75.0	10.5	5.0	1.5	--	--	7.0	--	565.0°C
Soda lime silicate (AR-Glas)	69.0	1.0	4.0	5.0	3.0	2.0	13.0	3.0	525.0°C

Table 2 $K_2O/(Na_2O+K_2O)$ molar ratio (%) on the tubes surface in different conditions: as bought raw glass, after ion exchange (IE), simply kept in the salt bath for 5 min and after E-Field assisted ion exchange (EF-IE)

	Raw glass	IE	5 min	EF-IE	
				Outer surface	Inner surface
Borosilicate	0	90	60	100	60
Soda lime silicate	10	80	80	100	60

Table 3 Average bending strength and corresponding standard deviation for raw glass tubes and samples subjected to conventional ion exchange (IE) and E-Field assisted ion exchange (EF-IE).

	Borosilicate			Soda Lime Silicate		
	Raw glass	IE	EF-IE	Raw glass	IE	EF-IE
Average strength (MPa)	64	122	137	122	387	199
Standard deviation (MPa)	18	17	36	26	74	63

Table 4 Relative concentration of Qn species in glass estimated from Raman spectra in Figure 9; numbers in parentheses show the random error cumulated upon fitting.

	Soda-Borosilicate		Soda-Lime Silicate	
	Bulk	Edge	Bulk	Edge
Q ₁	10.6(0.4)	8.4(0.8)	8.5(0.7)	8.7(0.0)
Q ₂	29.9(0.9)	24.9(0.3)	18.2(0.6)	13.9(0.1)
Q ₃	37.0(0.2)	44.7(0.1)	53.9(0.2)	59.6(0.1)
Q ₄	22.5(0.4)	22.1(0.0)	19.3(0.1)	17.8(0.1)